

Heavy metal adsorption of a novel membrane material derived from senescent leaves: Kinetics, equilibrium and thermodynamic studies

Yu Zhang¹, Qiang Tang^{*1,2,3}, Su Chen¹, Fan Gu⁴ and Zhenze Li⁵

¹School of Urban Rail Transportation, Soochow University, China

²Key Laboratory of Ministry of Education for Geomechanics and Embankment Engineering, Hohai University, China

³Jiangsu Research Center for Geotechnical Engineering Technology, Hohai University, China

⁴National Center for Asphalt Technology, Auburn University, USA

⁵Canadian Nuclear Safety Commission, Canada

(Received April 24, 2017, Revised July 9, 2017, Accepted July 10, 2017)

Abstract. Copper pollution around the world has caused serious public health problems recently. The heavy metal adsorption on traditional membranes from wastewater is limited by material properties. Different adsorptive materials are embedded in the membrane matrix and act as the adsorbent for the heavy metal. The carbonized leaf powder has been proven as an effective adsorbent material in removing aqueous Cu(II) because of its relative high specific surface area and inherent beneficial groups such as amine, carboxyl and phosphate after carbonization process. Factors affecting the adsorption of Cu(II) include: adsorbent dosage, initial Cu(II) concentration, solution pH, temperature and duration. The kinetics data fit well with the pseudo-first order kinetics and the pseudo-second order kinetics model. The thermodynamic behavior reveals the endothermic and spontaneous nature of the adsorption. The adsorption isotherm curve fits Sips model well, and the adsorption capacity was determined at 61.77 mg/g. Based on D-R model, the adsorption was predominated by the form of physical adsorption under lower temperatures, while the increased temperature motivated the form of chemical adsorption such as ion-exchange reaction. According to the analysis towards the mechanism, the chemical adsorption process occurs mainly among amine, carbonate, phosphate and copper ions or other surface adsorption. This hypothesis is confirmed by FT-IR test and XRD spectra as well as the predicted parameters calculated based on D-R model.

Keywords: carbonized leaf powder; membrane; Cu(II); adsorption; benefit groups; mechanism

1. Introduction

The presence of heavy metals in environment during the last decade aroused more public concern since their increasing discharge, toxic nature and other adverse effects to environmental ecosystem (Tang *et al.* 2015a). Heavy metals are not biodegradable and tend to accumulate in biological systems through food chain, and posing health hazards to human being if their concentrations exceed allowable limits (Bulgariu *et al.* 2009, Tang *et al.* 2016a). Among all highly toxic heavy metals, copper is a metal of great concern (Lin *et al.* 2013). Copper is an essential trace element for the healthy growth of living creatures, but at a higher concentration level, it is prone to be toxic. Intake of copper causes stomach and intestinal distress, kidney damage, and anemia (Carson *et al.* 1986). Thus, the Cu in drinking water is strictly regulated by most of countries, for example, according to the drinking water standard proposed by USEPA and Japan Ministry of Health, Labour and Welfare, the concentration of Cu(II) should be lower than 1.3 mg/L and 1.0 mg/L (USEPA 2009, Japan 2014). European Union, WHO and Australia recommend the upper limit of Cu(II) in drinking water is 2 mg/L (EU 1998,

Australia 2011, WHO 2011). Cu(II) contained wastewater is commonly produced during electroplating, PCB processing, mining, metallurgy, and battery manufacture (Gulnaz and Saygideger 2005). Besides, high concentrations of Cu(II) in landfill leachate also can be observed (Fan *et al.* 2006).

The conventional methods for heavy metal removal from wastewater include precipitation, ion exchange, oxidation, adsorption, coagulation, evaporation, redox, membrane filtration and extraction (Gavrilescu *et al.* 2009, Suteu *et al.* 2009). Membrane separations, as powerful tools for heavy metal removal, the performance of which is mainly limited by material properties (Kim and Bruggen 2010, Tang *et al.* 2015b). As an alternative technology, adsorption has been proven as an effective, versatile and simple method, and many polymeric and inorganic materials have been developed as adsorbents (Gavrilescu 2004, Xiong and Yao 2013, Fang *et al.* 2017). Recently, adsorptive membrane, which combines the advantages of membrane technology and adsorption process, has attracted a great deal of attention. Different adsorbent materials are incorporated with a polymeric membrane and act as the adsorbent for the heavy metals, which commonly known as hybrid membrane or mixed matrix membrane (Ghaemi *et al.* 2015, Zhu *et al.* 2015, Mukherjee *et al.* 2016). Commercial adsorbents are usually expensive, such as activated carbon. Thus, one intense debate focused on finding a material which has abundant deposit or relative

*Corresponding author, Ph.D.
E-mail: tangqiang@suda.edu.cn

low cost as the adsorbent, and this material should possess excellent and stable adsorption performance. According to previous researches, various activated carbon and unburned carbon were produced from low-cost materials in attempt to reduce the cost of carbon production, such as peat, sphagnum moss peat, cashew nut shell and fruit shell (Bulgariu *et al.* 2009, Kicsi *et al.* 2010, Kumar *et al.* 2014, Mondal *et al.* 2014). In this study, application of carbon made from a lost-cost agricultural waste, senescent leaf powder, for adsorption behavior towards Cu(II) was evaluated. The governing mechanisms are also discussed as well as several influencing factors including dosage, temperature, equilibration duration, solution pH, mineral component etc. Identification of the critical factors controlling adsorption process is one vitally important contribution to fully informing the development of effective strategies to manage waters worldwide.

2. Materials and experimental method

2.1 Preparation of the adsorbent and solutions

The senescent leaves were collected from the Yuquan campus of Zhejiang University. Most of them were firmiana simplex leaves. The collected leaves were oven dried at 105°C overnight and then pulverized in a mortar. The powder was placed on a ceramic plate which was then transferred into a muffle furnace (15×25×40 cm³). The temperature was regulated at 250°C, with an increment of 25-30°C/min, and then pertained for 5 h. There was no gas supply into the oven during the calcination process. The carbonized product was cooled to room temperature, and passed 24 mesh screen with diameters 355±13 μm. This product was designated as Carbonized Leaf Powder (CLP), and utilized in following test.

Stock solution was prepared by dissolving CuCl₂·2H₂O (ZHENXIN, China) in analytical grade into de-ionized water to 1 M standard solution, then stored in a refrigerator around 4°C. Before the test, the 1 M standard solution was diluted to the target concentrations for use. Conical flasks and PVC tubes (polyvinylchlorid centrifuge tubes) were immersed in 0.01 M HNO₃ solution overnight and then rinsed three times with de-ionized water.

2.2 Characterization

The specific surface area of CLP was determined by BET N₂ adsorption test (Autosorb 1-MP apparatus, Quantachrome Corporation, USA). The results were analyzed by using the BET adsorption theory to predict the specific surface area, volume of micropores and average pore size etc. FT-IR spectra of CLP and Cu(II) laden CLP were recorded using Fourier Transform Infrared Spectroscopy (Nexus-670, Nicolet, USA) to study the changes in the functional groups with respect to investigating the mechanism of Cu(II) adsorption. The pH of samples was measured by glass electrode potentiometer (pH 213, China). XRD spectra of CLP and Cu(II) laden CLP were obtained by D/MAX-RA diffractometer (Rigaku Corporation, Japan).

2.3 Experiment

2.3.1 Effect of adsorbent dosage

The adsorbent dosage (CLP) in the aqueous solution was increased from 0.5 to 1, 2, 5, 10 and 20 g/L. Three various initial Cu(II) concentration (50 mg/L, 100 mg/L and 200 mg/L) was set and transferred into stoppered conical flasks. After mixing with the adsorbent, the flasks were put into a thermostated agitator. Then, batch adsorption tests were conducted under isothermal conditions (25°C) for 24 h at 180 rpm without regulating the solution pH (THZ-C-1, BING, China). At the end, the mixture was separated by centrifuging at 3000 rpm for 5 min (TDZ5-WS, XIANGYI, China). The supernatant was collected and the equilibrium Cu(II) concentration was determined by Atomic Absorption Spectrophotometer (AAS) (TAS-990, PERSEE, China).

2.3.2 Adsorption kinetics

The adsorbent dosage was fixed 10 g/L and the initial solute concentrations were ranged from 50, 100 mg/L to 200 mg/L. The solution pH was not adjusted and the reaction temperature was maintained constant at 25°C. The test was stopped after specific times that increased from 3 to 6, 9, 12, 15, 20, 40, 80, 120, 180, 240, 300 and 1440 minutes. The mixture was transferred to PVC tubes and centrifuged at 3000 rpm for 3 min. The Cu(II) concentration in the supernatant was determined by AAS.

2.3.3 Adsorption isotherms and thermodynamics

The CLP (10 g/L) was blended with eight sets of copper chloride solution with increasing initial Cu(II) concentration from 25 to 600 mg/L (25, 50, 100, 200, 300, 400, 500 and 600 mg/L) at six sets of increased temperatures separately from 5 to 55°C with an increment of 10°C. Apart from this, some samples with other initial Cu(II) concentration (800 mg/L and 1, 2, and 5 g/L) at 55°C are also tested in order to obtain more details of adsorption capacity. All samples were equilibrated for 24 h in the controlled temperature agitator and the equilibrium Cu(II) concentrations were measured by AAS to calculate the amount on the adsorbent. Control and parallel samples were conducted in all above tests and the results were averaged.

2.3.4 Effect of pH

The same amount of CLP (400 mg) and Cu(II) solution (100 mg/L, 40 mL) were mixed and put into nine pretreated conical flasks (dosage, 10 g/L). Then pH_i, the initial solution pH, of these nine centrifuge tubes was adjusted ranged from 2.0 ± 0.2 to 10.0 ± 0.2 with an increment of 1.0 by adding 0.1 M HCl or NaOH solution. The sample flasks were then placed into a thermostated agitator (25°C) and rotated at 180 rpm for 24 h. The pH of solutions was measured at the end of the test. Afterwards, the solutions were transferred into PVC tubes for centrifugation at 3000 rpm for 5 min. The supernatants were sampled to determine the Cu(II) concentration by AAS.

3. Results and discussion

3.1 Characterization of the adsorbent

Based on the test results, the Specific Surface Area

(SSA) of CLP was determined at $6.26 \text{ m}^2/\text{g}$. The micropore and average pore diameter were determined at 14.0 and 20.0 \AA , respectively. The total pore volume reached $3.14 \times 10^{-3} \text{ cm}^3/\text{g}$. Compared to other reported porous materials such as activated carbons etc., the SSA of CLP is not encouraging. However, for CLP, the adsorption to inorganic toxicant does not depend merely on physical adsorption occurs at the pore space or surface areas. The reaction between the surface active sites and the objective heavy metals could contribute much more adsorption capacity than the physisorption on pore spaces. The following investigations confirmed these hypotheses as well as the effectiveness of the prepared material.

The FT-IR spectra of CLP before and after adsorption process in the range of $400\text{--}4000 \text{ cm}^{-1}$ were taken to obtain information on the adsorption mechanism and presented in Fig. 1. In general, the relevant functional groups on the samples could be determined based on the FT-IR adsorption band listed in Table 1. The weakness of band intensities of C-H group at 2920 and 2850 cm^{-1} shown in Fig. 1(a) mean that the C-H group content is very low after activation at 250°C (Zhao *et al.* 2010, Gao *et al.* 2013). The natural macromolecules (i.e., lignin) contained in the CLP, which remains stable even after mulched for 2 months (Jin *et al.* 2003), were greatly decomposed in this respect.

Amine groups were found in both samples according to the characteristic bands at wavenumber 1623 , 1319 and 475 cm^{-1} (Jones 1963). Compared with CLP, the band intensity of N-H in Cu(II) laden CLP shown in Fig. 1(b) was found decreased greatly after adsorption (1319 cm^{-1}), indicating the decreased percent of N-H group in the Cu(II) laden CLP sample. The band intensity at 1431 , 1119 and 875 cm^{-1} were found slightly decreased after the adsorption, suggesting the decreased proportion of the carboxyl group which is a preferential adsorption site for heavy metals (Tang *et al.* 2012). The weak band at 713 cm^{-1} was relevant either to hydrogen bonding with vanadyl group (Repelin *et al.* 1985) or to carbonate components (Jackson 1997).

In Fig. 1(a), the IR bands at 501 cm^{-1} relevant to phosphate (Somya *et al.* 2009) were observed in original CLP. Although some functions such as Si-O (781 cm^{-1}), O-H (3420 cm^{-1}) remain stable according to their band intensities, some new characteristic bands appeared after adsorption process (N-Cu at 1360 cm^{-1}), as shown in Fig. 1(b). More details will be discussed in adsorption mechanism in section 4.

Fig. 2 shows XRD spectra of CLP and Cu(II) laden CLP. In Fig. 2(a), the patterns at $2\theta=14.9^\circ$, 24.5° , 38.1° and 50.1° can be attributed to Whewellite (calcium oxalate hydrate). The pattern at $2\theta=24.5^\circ$ was sharp and strong, indicating that the crystalline of this component was well formed at 250°C . Characteristic bands at $2\theta=15.23^\circ$, 29.4° , 30.88° and 30.1° in spectrum (a) were assigned to sodium hydrogen phosphate hydrate and calcium hydroxide phosphate. Calcium phosphate also existed in CLP according to the related band at $2\theta=40.53^\circ$. The results also can be proved by characteristic band of phosphate observed in Fig. 1. The characteristic band related to calcite was at $2\theta=31.4^\circ$ and 35.9° , consisted with the discovery of carbonate in Fig. 1. Albite was associated with the band at $2\theta=28.3^\circ$. Quartz was regarded as abundant component in

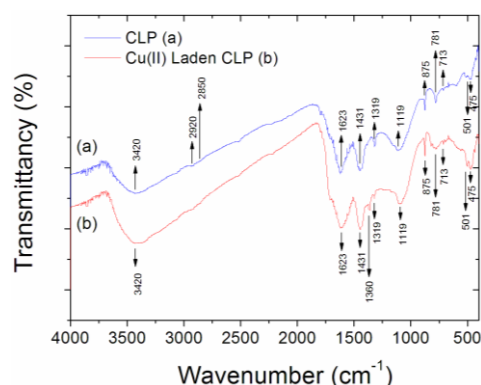


Fig. 1 FT-IR spectra of CLP and Cu(II) laden CLP

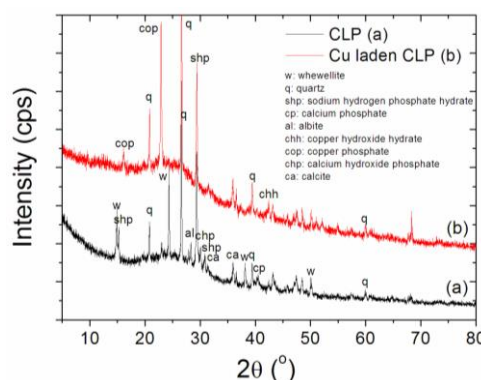


Fig. 2 XRD spectrum of CLP and Cu(II) laden CLP

Table 1 Band position in the FT-IR spectra

Sample		Assignment	References
CLP	Cu(II) laden CLP		
475	475	N-H	(Jones 1963)
	501	P=O	(Somya <i>et al.</i> 2009)
713	713	C=O	(Jackson 1997)
781	781	Si-O	
875	875	C=O	
1119	1119	C=O	
1319	1319	N-H	
	1360	N-Cu	(Casabo <i>et al.</i> 1983)
1431	1431	C=O	(Sangi <i>et al.</i> 2008)
1623	1623	N-H	
2850		C-H	
2920	2920	C-H	
3420	3420	OH	(Sinitnya <i>et al.</i> , 2000)

CLP through the bands at $2\theta=20.8^\circ$, 26.6° , 39.4° and 59.96° , in agreement with the presence of Si-O band in IR spectra as shown in Fig. 1 (Tang *et al.* 2014).

3.2 Adsorption studies

3.2.1 Effect of adsorbent dosage

The effect of adsorbent dosage on Cu(II) adsorption is shown in Fig. 3. It is apparent that although the total adsorption amount (Cu(II) removal from solution) rose as

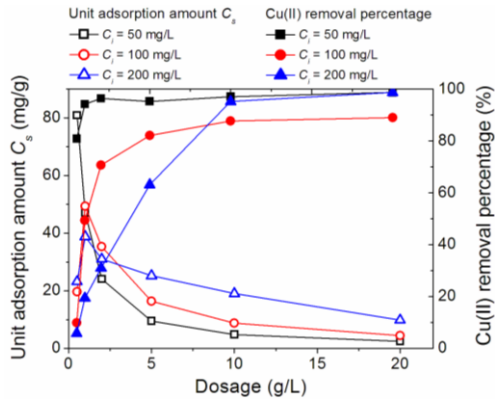


Fig. 3 Dosage effect on Cu(II) adsorption

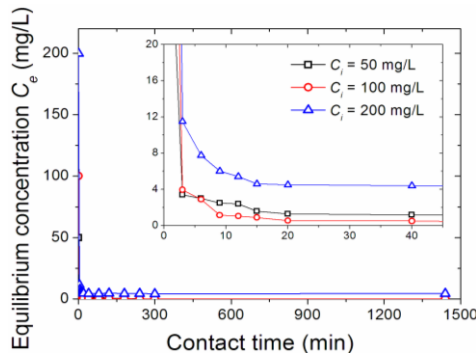


Fig. 4 Variation of concentration of Cu(II) with contact time

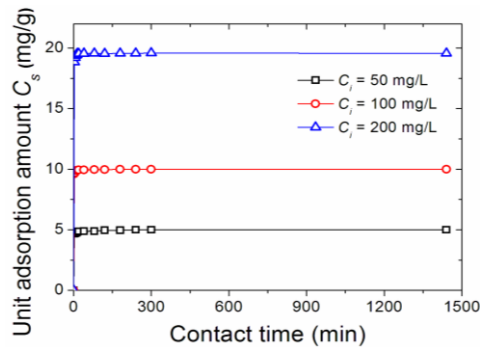


Fig. 5 Contact time effect on the unit adsorption amount

Table 2 Predicted kinetic constants of Cu(II) adsorption on CLP

C_i	Unit	50 mg/L	100 mg/L	200 mg/L
The pseudo-first order kinetics equation				
Q_e	mg/g	4.89	9.94	19.52
k_1	min^{-1}	0.99	1.12	1.12
R^2		0.99	0.99	0.99
The pseudo-second order kinetic equation				
k_2	$\text{g/mg}\cdot\text{min}$	0.84	0.77	0.45
Q_e	mg/g	4.94	10.00	19.61
R^2		0.99	0.99	0.99
The equation on the intraparticle diffusion model				
k_{int}	$\text{mg/g}\cdot\text{min}^{1/2}$	0.009	0.007	0.009
C		4.78	9.85	19.37
R^2		0.55	0.30	0.19

the dosage increased, the unit adsorption amount of the CLP decreased continually, this phenomenon may be due to the saturation of the biosorbent surface (Nemeş and Bulgariu 2016). But this trend was not linear, as the great decline at the first stage was interrupted and what followed became flat gradually at higher dosage. In addition, similar to Kovalchuk *et al.* (2001), we find that when initial Cu(II) concentration are high (i.e., $C_i=100$ mg/L and $C_i=200$ mg/L) as well as the low dosage (0.5 g/L), the unit adsorption amount towards Cu(II) would be lower, maybe the strong acidity of the Cu(II) solution prevent or weaken the adsorption process, and the effect of pH will be discussed in section 4.

3.2.2 Adsorption kinetics

The variation of concentration of Cu(II) with contact time at different initial Cu(II) concentrations is shown in Fig. 4. The contact time for equilibrium was found increased with increasing initial Cu(II) concentration. The equilibration duration is determined to be only about 3 min, when $C_i=50$ mg/L, but as initial Cu(II) concentration increases, 9 min and 15 min will be required when $C_i=100$ and 200 mg/L respectively. It is noteworthy to mention that the duration required to reach equilibrium in this study is far less than that of other adsorbent in previous study (Tang *et al.* 2009).

Fig. 5 plots q of Cu(II) on CLP as a function of contact time. From the chart, it is obvious that the unit adsorption amount of Cu(II) reaches a relative high value within a fairly short time (less than 3 min) and then slowly increases until it reaches a plateau after 40 min. The test data were further analyzed using three kinetic models as follows (pseudo-first order kinetics, pseudo-second order kinetics and intraparticle diffusion model) (Naiya *et al.* 2009, Anbia *et al.* 2015). The pseudo-first order kinetic equation can be written as

$$\lg(Q_e - q) = \lg(C_e) - \frac{k_1}{2.303}t \quad (1)$$

where Q_e and q are the amount of solute adsorbed per unit adsorbent at equilibrium and any time, respectively (mg/g), and k_1 the pseudo-first order rate constant (min^{-1}). The pseudo-second order kinetic equation is

$$\frac{t}{q} = \frac{1}{k_2 Q_e^2} + \frac{1}{Q_e}t \quad (2)$$

where k_2 is the pseudo-second order rate constant ($\text{g/mg}\cdot\text{min}$). The equation on the intraparticle diffusion model is

$$q = k_{\text{int}}t^{1/2} + C \quad (3)$$

where k_{int} is the relevant rate constant ($\text{mg/g}\cdot\text{min}^{1/2}$) and C is the intercept.

Table 2 lists the critical parameters of adsorption kinetics. From the correlation coefficient values listed in the table, we could easily judge that both the pseudo-first order kinetics equation ($R^2=0.99, 0.99$ and 0.99) and the pseudo-second order kinetic equation ($R^2=0.99, 0.99$ and 0.99) could fit the test data well. Besides, there was a slight

decrease in the rate constant k_2 from 0.836, 0.767 to 0.445 g/mg·min when increasing the initial Cu(II) concentration from 50 to 200 mg/L. This indicated that the solution with the smallest solute concentration is likely to reach equilibrium most quickly. This phenomenon is consistent with our common sense and has been previously observed for Pb(II) adsorption on natural Kaolin (Tang *et al.* 2009).

3.2.3 Adsorption Isotherms

As shown in Fig. 6, the unit adsorption amount of Cu(II) shows a gradual ascending trend and eventually achieved a maximum adsorption amount with increased equilibrium solute concentrations. Three two-parameter isothermal models (Langmuir, Freundlich, and D-R models) and two three-parameter models (Redlich-Peterson and Sips models) were applied to evaluate the test results in order to provide more information on adsorption mechanisms. The Langmuir isotherm can be written as (Faghian and Rasekh 2014)

$$\frac{1}{q} = \frac{1}{Q^0} + \frac{1}{bQ^0C_e} \quad (4)$$

where C_e is the equilibrium concentration of solute solution (mg/L), Q^0 the maximum adsorption capacity of the adsorbent (mg/g), and b (L/mg) the Langmuir constant.

The Freundlich model stipulates that the ratio of solute adsorbed from the solute concentration is a function of the equilibrium concentration of solute solution, which can be expressed as

$$q = K_F C_e^{1/n} \quad (5)$$

where K_F is the Freundlich constant (mg/g) indicating the adsorption capacity and strength of the adsorptive bond, and n the heterogeneity factor.

The D-R model assumes a uniform pore-filling sorption and can predict the free sorption energy change by which the sorption type can be judged (Gulnaz and Saygideger 2005, Uslu and Tanyol 2006). The D-R model is written as

$$\ln q = \ln q_m - k\varepsilon^2 \quad (6)$$

where q_m is the maximum adsorption capacity (mol/g), k is a model constant related to the free sorption energy and ε is the Polanyi potential, which is written as

$$\varepsilon = RT \ln(1 + (1/C_e)) \quad (7)$$

The mean free energy of adsorption (E) is

$$E = -\frac{1}{\sqrt{2k}} \quad (8)$$

The adsorption is basically a surface chemical adsorption such as ion exchange when $|E|$ is between 8 and 16 kJ/mol. Otherwise, for $|E|$ ranging 1.0 - 8.0 kJ/mol, it suggested the occurrence of physical adsorption (Helfferich 1962).

The Redlich-Peterson model can be applied either in homogeneous or heterogeneous systems due to its versatility, which is expressed as (Redlich and Peterson 1959)

$$q_e = \frac{K_{RP} C_e}{1 + \alpha_{RP} C_e^\beta} \quad (9)$$

where K_{RP} (L/g) and α_{RP} (L/mg) $^\beta$ are Redlich-Peterson model constants and β is the exponent which lies between 0 and 1.

Sips model is a combined form of Langmuir and Freundlich expressions deduced for predicting the heterogeneous adsorption systems (Sips 1948). At low

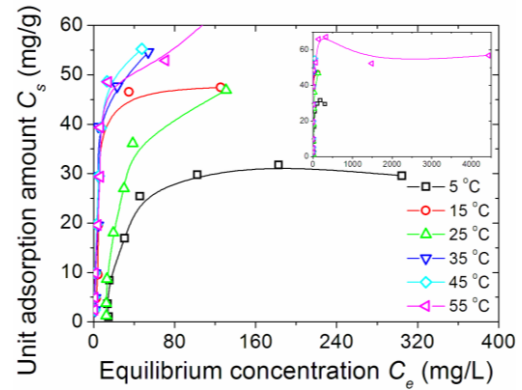


Fig. 6 Isothermal adsorption lines under different temperatures

Table 3 Predicted constants of isothermal models for Cu(II) adsorption

Temperature	Unit	278 K	288 K	298 K	308 K	318 K	328 K
Langmuir model							
Q^0	mg/g	39.20	54.31	64.53	62.42	65.64	66.72
b	L/mg	0.02	0.13	0.02	0.15	0.17	0.14
R^2		0.85	0.81	0.91	0.86	0.97	0.97
Freundlich model							
K_F	mg/g	3.50	12.39	2.50	12.30	13.86	16.75
n		2.46	3.27	1.62	2.52	2.57	3.82
R^2		0.71	0.64	0.77	0.76	0.84	0.84
D-R model							
q_m	mg/g	281.73	391.87	2250.57	709.84	684.12	242.53
k	mol ² /kJ ²	0.011	0.007	0.014	0.006	0.006	0.004
E	kJ/mol	-6.71	-8.70	-6.04	-8.91	-9.54	-11.32
R^2		0.65	0.68	0.66	0.73	0.87	0.86
Redlich-Peterson model							
K_{RP}	L/g	0.80	7.16	1.07	9.49	10.89	10.86
α_{RP}	(L/mg) $^\beta$	0.020	0.133	0.014	0.152	0.166	0.183
β		1	1	1	1	1	1
R^2		0.85	0.80	0.84	0.86	0.97	0.95
Sips model							
q_{ms}	mg/g	30.14	44.52	48.67	51.94	57.73	61.77
K_s	(L/mg) ms	7.0E-5	7.0E-09	9.0E-5	5.3E-2	0.112	0.101
m_s		2.89	12.10	2.86	2.14	1.46	1.30
R^2		0.98	0.96	0.98	0.92	0.99	0.97

concentrations, it reduces to Freundlich isotherm; while at high concentrations, it predicts a monolayer adsorption form of the Langmuir isotherm

$$q_e = \frac{q_{mS} K_S C_e^{m_S}}{1 + K_S C_e^{m_S}} \quad (10)$$

where q_{mS} is the Sips maximum adsorption capacity (mg/g), K_S is the Sips equilibrium constant (L/mg) ^{m_S} , and m_S is the Sips model exponent.

The results of predicted isothermal constants for the adsorption of Cu(II) are gathered in Table 3. It is apparent that Sips model shows the best-fit to the test data based on calculated correlation coefficients, most of which in Sips model are higher than 0.95, which means the parameters could be measured more accurately through Sips models. According to Sips model results, the predicted Cu(II) adsorption capacities of CLP are found to increase from 30.14 to 61.77 mg/g with increasing temperature from 278 to 328 K, respectively. The Langmuir model also fits the test data well, in which most correlation coefficients are higher than 0.85. According to Langmuir model, adsorption occurs uniformly on the active sites of the adsorbent, and once adsorbate occupies a site, no further adsorption can take place at this site (Akar *et al.* 2005). Similarly, to Unuabonah (Unuabonah *et al.* 2007), we found that adsorption capacity towards Cu(II) came to the peak point at the highest temperature condition according to the above data.

The adsorption capacities estimated by D-R model were considerably higher than those obtained from Sips and Langmuir models since the inherent assumption in the D-R model that all micropores are filled with solute. However, this ideal state is difficult to realize in practice. According to the D-R model, the absolute values of most estimated free adsorption energy had a graduate increase along with the temperature, less than 8 kJ/mol when temperatures were relative low and higher than 8 kJ/mol as the temperature increased. Such a fluctuation of free adsorption energy indicated that under lower temperatures, the adsorption was predominated by the form of physical adsorption, while the increased temperature motivated the form of chemical adsorption such as ion-exchange reaction.

3.2.4 Thermodynamics

For the sake of studying the thermodynamic behaviors of Cu(II) adsorption, thermodynamic considerations were evaluated. Thermodynamic parameters such as enthalpy change (ΔH^0), Gibb's free energy change (ΔG^0) and entropy change (ΔS^0) can be estimated with the following Gibb's free energy equations

$$\Delta G^0 = -RT \ln K_D \quad (11)$$

$$\Delta G^0 = \Delta H^0 - T\Delta S^0 \quad (12)$$

where R is the ideal gas constant (8.314 J/mol·K), T the absolute temperature (K), K_D is the distribution coefficient of the solute between the adsorbent and the solution in equilibrium q/C_e (mL/g). Eqs. (11) and (12) can be written in a linearized form between K_D and $1/T$ as

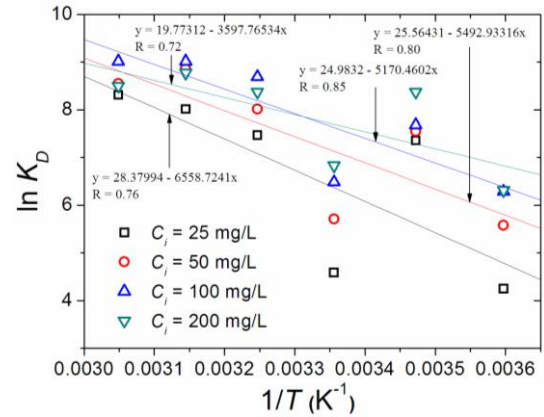


Fig. 7 Fitting test data with Gibb's free energy equations

Table 4 Thermodynamic parameters for adsorption of Cu(II) on CLP

Temperature	C _i	Unit	25 mg/L	50 mg/L	100 mg/L	200 mg/L
			G ⁰	G ⁰	G ⁰	G ⁰
278 K		kJ/mol	-9.82	-12.90	-14.54	-14.60
288 K		kJ/mol	-17.62	-18.08	-18.40	-20.06
298 K		kJ/mol	-11.37	-14.16	-16.08	-16.92
308 K		kJ/mol	-19.12	-20.52	-22.26	-21.45
318 K		kJ/mol	-21.19	-23.42	-23.84	-23.19
328 K		kJ/mol	-22.66	-23.31	-24.59	-23.17
ΔS^0		J/mol·K	235.95	212.54	207.71	164.39
ΔH^0		kJ/mol	54.53	45.67	42.99	29.91
R			0.76	0.80	0.85	0.72

$$\ln K_D = \frac{\Delta S^0}{R} - \frac{\Delta H^0}{RT} \quad (13)$$

Values of ΔH^0 and ΔS^0 can be determined from the slope and the intercept of the plot between $\ln K_D$ versus $1/T$.

The predicted constants of thermodynamics shown in Table 4 can be determined through linearization of the test data as shown in Fig. 7. The calculated Gibb's free energy decreased along with an increasing reaction temperature at a fixed initial solute concentration. Moreover, the Gibb's free energy was negative, which suggested that the adsorption process was spontaneous and could be promoted by the increasing temperature, which is the reason why adsorption capacity came to peak point at highest temperature according to Sips isotherm. With increasing initial Cu(II) concentration, the Gibb's free energy for Cu(II) adsorption decreased under constant temperature conditions. The change of enthalpy was 54.53, 45.67, 42.99, 29.91 kJ/mol and the change of entropy was 235.95, 212.54, 207.71 and 164.39 J/mol·K when the initial Cu(II) concentration increased from 25 to 50, 100 and 200 mg/L respectively, which implies an endothermic character to the adsorption process and increasing disorder in the system.

3.2.5 Effect of pH

Fig. 8 plots Cu(II) adsorption percent on CLP versus the

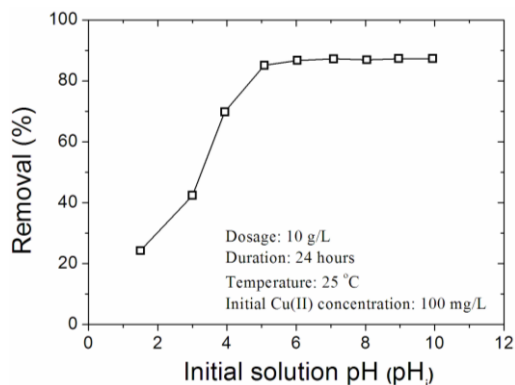


Fig. 8 Variation of Cu(II) removal percentage with varied initial solution pH (pH_i)

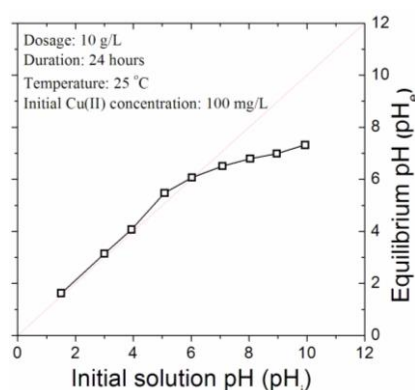


Fig. 9 Variation of equilibrium pH (pH_e) under different initial solution pH (pH_i)

initial solution pH (pH_i). A sharp pH-adsorption edge could be observed between pH 2.0 and 5.0, while the percentage Cu(II) removal boosts from 30.2% to 85.1%, the curve then plateaus at 87.3% Cu(II) removal with continuously increasing pH_i. In addition, we could find that most of copper ions (85.1%) have been removed while the solution is highly acid (pH_i=5.08). However, after pH_i reached 5, enhancing the alkalinity of solution would lead no more Cu(II) removal, namely, raising the solution pH merely do not promote the Cu(II) adsorption. This phenomenon will be discussed in the next section.

Fig. 9 shows that equilibrium pH (pH_e) values approximately lie on the diagonal line at pH_i<6.07 and below the diagonal at 6.07≤pH_i<9.94. It is obvious that the CLP owns good buffering capability which could resist pH changes effectively, especially for solution at pH>6.07. This effect failed in solution at pH<6.07. The changing pattern of pH_e might reflect the inherent mechanism that governing the adsorption of Cu(II) on CLP, particularly regarding the effect of solution pH.

4. Discussions

Fig. 1 shows the FT-IR spectra of CLP before and after Cu(II) adsorption. The characteristic IR band could be assigned to specific functional group as shown in Table 1. The band at 713, 875, 1119 and 1431 cm⁻¹ in the IR

spectrum of CLP was assigned to carbonate component, corresponding to the calcite content identified by the XRD spectra (2θ=28.3°) as shown in Fig. 2. With respect to that calcite had been proved to be a kind of effective adsorbent to remove heavy metals from solutions (Tang *et al.* 2010), the adsorption of Cu(II) on CLP may be written as

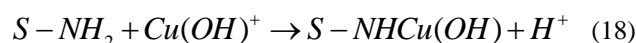
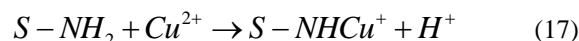


This is a typical ion-exchange adsorption and could be linked to the results of D-R analysis, which indicates the presence of chemical adsorption. However, as to CLP, the intensity of the band relevant to carbonate had no obvious change after Cu(II) adsorption, suggesting that the carbonate contained in CLP was not the dominant adsorption site for Cu(II).

The bands at 475, 1319 and 1623 cm⁻¹ could be assigned to the vibration of N-H group. Amine group was reported as a significant binding site for metal uptake in biosorbents (Kilic *et al.* 2008). As an alkaline functional group, amine could give rise to the solution pH. In this study, the equilibrium pH of the adsorbent/water slurry (10 g/L) was higher than 8.60, corresponding to the presence of alkaline component in CLP. The high affinity of amine towards Cu(II) would contribute to the adsorption of Cu(II) on CLP. However, the deprotonated amine group would turn to possess positive charges at pH<2.0. This behavior might pronouncedly reduce the Cu(II) adsorption capacity, which could explain the minor removal percent (24.2%) at solution pH=1.50 and the sharp pH adsorption edge between 2.0 - 5.0 observed in Fig. 8 and Fig. 9. Moreover, Cu(II) solution presented acidity as a result of the follow equation



Both of the two equations have been proved by the existence of Cu(OH)₂ according to XRD as shown in Fig. 2. The highly acidity of Cu(II) solution affects the adsorption character of CLP, maybe it is the reason why unit adsorption amount at lower Cu(II) concentration is higher as mentioned in 3.2.1. Furthermore, the N-H IR intensities were significantly weakened during the Cu(II) adsorption process as shown in Fig. 1. More exactly, the disappearance of some N-H group indicates the following reaction



Eqs. (15) and (16) as well as Eqs. (17) and (18), would be regarded as a good explanation why pH always dropped (pH_i > pH_e) after Cu(II) adsorption especially when pH>6.0. Eq. (18) was also proved by the FT-IR spectra in which the band related to O-H (3420 cm⁻¹) kept stable throughout the test.

The main minerals in CLP are quartz, whewellite, albite and phosphate as determined from the characteristic bands on the XRD spectra (see Fig. 2). New patterns were

Table 5 Reported adsorption capacity of Cu(II) on various adsorbents

Materials	Adsorption capacity	Reaction time	References
<i>Fucus vesiculosus</i>	105.41 mg/g		(Mata <i>et al.</i> 2008)
<i>Fucus serratus</i>	101.6 mg/g		(Ahmady-Asbchin <i>et al.</i> 2008)
<i>Bacillus subtilis</i> immobilized on chitosan	100.7 mg/g		(Wang and Chen 2013)
<i>Candida Tropicalis</i> (yeast)	80 mg/g		(Figueroa-Torres <i>et al.</i> 2016)
CLP	61.77 mg/g	5 - 10 min	This study
Rice husk	29 mg/g	120 min	(Wong <i>et al.</i> 2003)
Banana pith	13.46 mg/g	20 min	(Low <i>et al.</i> 1995)
Sugar beet pulp	28.5 mg/g	60 min	(Aksu and Isoglu 2005)
Papaya wood	19.88 mg/g	30 min	(Saeed <i>et al.</i> 2005)
Tobacco dust	36 mg/g	90 min	(Qi and Aldrich 2008)
Olive stone waste	2.04 mg/g	60 min	(Fiol <i>et al.</i> 2006)

observed at $2\theta=16.17^\circ$, 22.92° and 42.41° compared with original CLP, however, the patterns at $2\theta=14.9^\circ$, 15.23° , 24.5° , 28.3° , 30.1° , 30.88° , 38.1° and 40.53° disappeared when the CLP was loaded with Cu(II). The patterns at $2\theta=16.17^\circ$ and 22.92° can be attributed to $\text{Cu}_3(\text{PO}_4)_2$ and the patterns at $2\theta=42.41^\circ$ the patterns can be attributed to $\text{Cu}(\text{OH})_2$ according to the MDI Jade software.

The presence of phosphate (at $2\theta=15.23^\circ$, 29.4° , 30.1° , 30.88° and 40.53° as exhibited in Fig. 2) would contribute to the adsorption of Cu(II) in the form as follows



In terms that the component of MHPO_4 in the adsorbent was soluble. And the appearance of $\text{Cu}_3(\text{PO}_4)_2$ verifies the existence of Eq. (20). It is noteworthy to mention that if the cation M was magnesium, the Eq. (19) reaction will become insignificant with respect to its comparatively low dissolution coefficients. In addition, whewellite (calcium oxalate) maybe play an important part in metal adsorption since the disappearance of related band in XRD spectra (at $2\theta = 14.9^\circ$, 24.5° and 38.1°), as suggested previously by Singer *et al.* (Singer *et al.* 2008).

Various biosorbents have been investigated with respect to Cu(II) adsorption performance. Table 5 shows the Cu(II) adsorption capacities of some recently reported biosorbents. It is seen that adsorption potential of CLP was lower compared to other biomass. Nevertheless, for the industrialization of wastewater treatment, the implementation of biosorption still has some difficulties. It is mainly due to the relatively weak growth ability of microorganisms in the natural state and its poor impact resistance, which limits its wide application in industry. However, the adsorption potential of CLP was better than that of many natural/unmodified alternate adsorbents reported in the literature. As shown in Table 5, the CLP has a relatively high adsorption capacity towards Cu(II), and meanwhile, it has the fastest rate of reaction among the reported biological materials (e.g., rice husk, banana pith, sugar beet pulp, papaya wood, tobacco dust and olive stone

waste). As a promising adsorbent material, CLP also contains excellent adsorption capacity towards most major heavy metal ions. According to Tang *et al.* (2016b, 2012, 2010), Firmiana simplex leaves were evaluated for its adsorption performance towards Ni(II), Zn(II) and Cd(II). The results presented that the senescent leaf powder appears prominent in Ni(II) removal from aqueous solution and the adsorption capacity of CLP towards Ni(II), Zn(II) and Cd(II) are determined at 37.62 mg/g, 55.096 mg/g and 117.786 mg/g, respectively. Li *et al.* (2009) proposed a simple activation method to mineralize the Firmiana Simplex leaf into an enhanced adsorbent for Pb(II) removal from aqueous solution. It was found that the adsorbent activated at 200°C was found most suitable for Pb(II) adsorption regarding the high yield efficiency (36.52%), high Pb(II) adsorption capacity (136.7 mg/g by Langmuir model), high adsorption affinity (H type isotherm) and rapid adsorption rate (within 20 min by kinetic study). Besides, as a widely planted tree, the Firmiana Simplex provides a locally available cheap source of adsorbent. The activation method provided here proves effective and appears promising in the heavy metals removal from wastewaters.

5. Conclusions

1) CLP studied in this paper appeared prominent in Cu(II) removal from aqueous solution and exhibited promising potential of application in industry. The determined adsorption capacity of CLP towards Cu(II) was 61.77 mg/g. Moreover, this also solved the problem of senescent leaves waste in future.

2) The required reaction time for equilibrium was about 3 min while initial Cu(II) concentration was raised from 50 to 200 mg/L, and the kinetics data were well fitted using pseudo-first order kinetics equation and the pseudo-second order kinetic equation with high correlation coefficients close to 1.0.

3) In terms of the correlation coefficients, the Sips model was the best model, which has correlation coefficients greater than 0.95; Langmuir model also fit test data well, which has correlation coefficients greater than 0.85.

4) The fluctuation of free adsorption energy predicted by D-R model indicated that the adsorption for CLP was originated from both physical bond and chemical adsorption. The adsorption of Cu(II) on CLP could be viewed as an endothermic and a preferential process with enthalpy change at around 45 kJ/mol. The negative Gibb's free energy changes implied a spontaneous adsorption procedure.

5) According to the analysis to XRD and FT-IR results, the chemical adsorption mainly occurred among copper ions and amine, carbonate, phosphate, which was benefit to the process. Thereby, CLP is a promising adsorbent material, which can be developed to prepare the adsorptive membrane by embedded in the membrane matrix and act as an adsorbent for the heavy metal.

Acknowledgments

The research presented herein is supported by the National Nature Science Foundation of China (50879023,

41630633), China Postdoctoral Science Foundation funded project (2016M591756), Jiangsu Planned Projects for Postdoctoral Research Funds (1601175C), and project from Jiangsu Provincial Department of Housing and Urban-Rural Development (2016ZD18). The research is also supported by Jiangsu Provincial Transport Bureau (2016T05) and Bureau of Housing and Urban-Rural Development of Suzhou.

References

- Ahmady-Asbchin, S., Andr s, Y., G rente, C. and Cloirec, P.L. (2008), "Biosorption of Cu(II) from aqueous solution by fucus serratus: Surface characterization and sorption mechanisms", *Bioresour. Technol.*, **99**(14), 6150-6155.
- Akar, T., Tunali, S. and Kiran, I. (2005), "Botrytis cinerea as a new fungal biosorbent for removal of Pb(II) from aqueous solutions", *Biochem. Eng. J.*, **25**(3), 227-235.
- Aksu, Z. and Isoglu, I.A. (2005), "Removal of copper(II) ions from aqueous solution by biosorption onto agricultural waste sugar beet pulp", *Proc. Biochem.*, **40**, 3031-3044.
- Anbia, M., Kargosha, K. and Khoshbooei, S. (2015), "Heavy metal ions removal from aqueous media by modified magnetic mesoporous silica MCM-48", *Chem. Eng. Res. Des.*, **93**, 779-788.
- Bulgariu, L., Ratoi, M., Bulgariu, D. and Macoveanu, M. (2009), "The sorption of lead(II) ions from aqueous solutions on peat: Kinetics study", *Environ. Eng. Manage. J.*, **8**(2), 289-295.
- Carson, B.L., Ellis, H.V. and Mccann, J.L. (1987), "Toxicology and biological monitoring of metals in humans", *Quarter. Rev. Biol.*, **62**(4), 259.
- Casabo, J., Izquierdo, M., Ribas, J. and Diaz, C. (1983), "Copper(II) complexes with derivatives of 8-Aminoquinoline", *Trans. Met. Chem.*, **8**(2), 110-113.
- EU (2014), *European Drinking Water Directive*, European Commission, European Union, <<http://ec.europa.eu/environment/water/water-drink/>>.
- Faghihian, H. and Rasekh, M. (2014), "Removal of chromate from aqueous solution by a novel clinoptilolite-polyanillin composite", *Iran. J. Chem. Chem. Eng.*, **33**(1), 45-51.
- Fan, H.J., Shu, H.Y., Yang, H.S. and Chen, W.C. (2006), "Characteristics of landfill leachates in central Taiwan", *Sci. Total Environ.*, **361**(1-3), 25-37.
- Fang, X.F., Li, J.S., Li, X., Pan, S.L., Zhang, X., Sun, X.Y., Shen, J.Y., Han, W.Q. and Wang, L.J. (2017), "Internal pore decoration with polydopamine nanoparticle on polymeric ultrafiltration membrane for enhanced heavy metal removal", *Chem. Eng. J.*, **314**, 38-49.
- Figuroa-Torres, G.M., Certucha-Barrag n, M.T., Acedo-F elix, E., Monge-Amaya, O., Almdariz-Tapia, F.J. and Gasca-Estefan a, L.A. (2016), "Kinetic studies of heavy metals biosorption by acidogenic biomass immobilized in clinoptilolite", *J. Taiwan Inst. Chem. Eng.*, **61**, 241-246.
- Fiol, N., Villaescusa, I., Mart nez, M., Miralles, N., Poch, J. and Serarols, J. (2006), "Sorption of Pb(II), Ni(II), Cu(II) and Cd(II) from aqueous solution by olive stone waste", *Sep. Purif. Technol.*, **50**(1), 132-140.
- Gao, Y., Gu, F., and Zhao, Y. (2013), "Thermal oxidative aging characterization of SBS modified asphalt", *J. Wuhan Univ. Technol. Mater. Sci.*, **28**(1), 88-91.
- Gavrilescu, M. (2004), "Removal of heavy metals from the environment by biosorption", *Eng. Life Sci.*, **4**(3), 219-232.
- Gavrilescu, M., Pavel, L.V. and Cretescu, I. (2009), "Characterization and remediation of soils contaminated with uranium", *J. Hazard. Mater.*, **163**(2-3), 475-510.
- Ghaemi, N., Madaeni, S.S., Daraei, P., Rajabi, H., Zinadini, S., Alizadeh, A., Heydari, R., Beygzadeh, M. and Ghousivand, S. (2015), "Polyethersulfone membrane enhanced with iron oxide nanoparticles for copper removal from water: Application of new functionalized Fe₃O₄ nanoparticles", *Chem. Eng. J.*, **263**, 101-112.
- Gulnaz, O. and Saygideger, S.E. (2005), "Study of Cu(II) biosorption by dried activated sludge: Effect of physico-chemical environment and kinetics study", *J. Hazard. Mater.*, **120**(1-3), 193-200.
- Helfferich, F. (1962), *Ion Exchange*, McGraw-Hill, New York, U.S.A.
- Jackson, K.D. (1997), "A guide to identifying common inorganic fillers and activators using vibrational spectroscopy", *J. Rubber Res.*, **12**(2), 102-111.
- Jin, Z., Akiyama, T., Chung, B.Y., Matsumoto, Y., Iiyama, K. and Watanabe, S. (2003), "Changes in lignin content of leaf litters during mulching", *Phytochem.*, **64**(5), 1023-1031.
- Jones, R.A. and Pyrrole Studies, I. (1963), "The infrared spectra of 2-monosubstituted pyrroles", *Austr. J. Chem.*, **16**(1), 93-100.
- Kicsi, A., Bilba, D. and Macoveanu, M. (2010), "Equilibrium and kinetic modeling of Zn (II) sorption from aqueous solutions by sphagnum moss peat", *Environ. Eng. Manage. J.*, **9**(3), 341-349.
- Kilic, M., Keskin, M.E., Mazlum, S. and Mazlum, N. (2008), "Hg(II) and Pb(II) adsorption on activated sludge biomass: Effective biosorption mechanism", *J. Min. Proc.*, **87**(1-2), 1-8.
- Kim, J. and Bruggen, B.V.D. (2010), "The use of nanoparticles in polymeric and ceramic membrane structures: Review of manufacturing procedures and performance improvement for water treatment", *Environ. Pollut.*, **158**(7), 2335-2349.
- Kovalchuk, O., Titov, V., Hohn, B. and Kovalchuk, L. (2001), "A sensitive transgenic plant system to detect toxic inorganic compounds in the environment", *Nat.*, **19**(6), 568-572.
- Kumar, P.S., Abhinaya, R.V., Arthi, V., Lashmi, K.G., Priyadarshini, M. and Sivanesan, S. (2014), "Adsorption of methylene blue dye onto surface modified cashew nut shell", *Environ. Eng. Manage. J.*, **13**(3), 545-556.
- Li, Z.Z., Tang, X.W., Chen, Y.M. and Wang, Y. (2009), "Activation of Firmiana simplex leaf and the enhanced Pb(II) adsorption performance: Equilibrium and kinetic studies", *J. Hazard. Mater.*, **169**(1-3), 386-394.
- Lin, L., Liu, G.G., Lv, W.Y., Yao, K., Lin, Q.T. and Zhang, Y. (2013), "Removal of chelated copper by TiO₂ photocatalysis: Synergistic mechanism between Cu (II) and organic ligands", *Iran. J. Chem. Chem. Eng.*, **32**(1), 103-112.
- Low, K.S., Lee, C.K. and Leo, A.C. (1995), "Removal of metals from electroplating wastes using banana pith", *Bioresour. Technol.*, **51**(2-3), 227-231.
- Mata, Y.N., Bl zquez, M.L., Ballester, A., Gonz lez, F. and Mu oz, J.A. (2008), "Characterization of the biosorption of cadmium, lead and copper with the brown alga fucus vesiculosus", *J. Hazard. Mater.*, **158**(2-3), 316-323.
- Ministry of Health, Labour and Welfare (2014), *Regulations of Drinking Water*, Ministry of Health, Labour and Welfare, Japan, <<http://www.mhlw.go.jp/stf/seisakunitsuite/bunya/topics/bukyo/ku/kenkou/suido/kijun/kijunchi.html>>.
- Mondal, P.K., Ahmad, R. and Kumar, R. (2014), "Adsorptive removal of hazardous methylene blue by fruit shell of cocus nucifera", *Environ. Eng. Manage. J.*, **13**(2), 231-240.
- Mukherjee, R., Bhunia, P. and De, S. (2016), "Impact of graphene oxide on removal of heavy metals using mixed matrix membrane", *Chem. Eng. J.*, **292**, 284-297.
- Naiya, T.K., Bhattacharya, A.K., Mandal, S. and Das, S.K. (2009), "The sorption of lead(II) ions on rice husk ash", *J. Hazard. Mater.*, **163**(2-3), 1254-1264.
- Neme , L. and Bulgariu, L. (2016), "Optimization of process parameters for heavy metals biosorption onto mustard waste

- biomass”, *Open Chem.*, **14**(1), 175-187.
- NHMRC (2011), *Australian Drinking Water Guidelines Paper 6 National Water Quality Management Strategy*, National Health and Medical Research Council, National Resource Management Ministerial Council, Commonwealth of Australia, Canberra, Australia, 7-5.
- Qi, B.C. and Aldrich, C. (2008), “Biosorption of heavy metals from aqueous solutions with tobacco dust”, *Bioresour. Technol.*, **99**(13), 5595-5601.
- Redlich, O. and Peterson, D.L.A. (1959), “Useful adsorption isotherm”, *J. Phys. Chem.*, **63**(6), 1024-1026.
- Repelin, Y., Husson, E., Abello, L. and Lucazeau, G. (1985), “Structural study of gels of V₂O₅: Normal coordinate analysis”, *Spectrochimica Acta Part A Molecul. Spectroscop.*, **41**(8), 993-1003.
- Saeed, A., Akhtar, M.W. and Iqbal, M. (2005), “Removal and recovery of heavy metals from aqueous solution using papaya wood as a new biosorbent”, *Sep. Purif. Technol.*, **45**(1), 25-31.
- Sangi, M.R., Shahmoradi, A., Zolgharnein, J., Azimi, G.H. and Ghorbandoost, M. (2008), “Removal and recovery of heavy metals from aqueous solution using ulmus carpinifolia and fraxinus excelsior tree leaves”, *J. Hazard. Mater.*, **155**(3), 513-522.
- Singer, D.M., Johnson, S.B., Catalano, J.G., Farges, F. and Brown Jr., G.E.B. (2009), “Sequestration of sr(ii) by calcium oxalate-a batch uptake study and exafs analysis of model compounds and reaction products”, *Geochimica Cosmochimica Acta*, **72**(20), 5055-5069.
- Sinitnya, A., ČopíKová, J., Prutyánov, V., Skoblyá, S. and Machovič, V. (2000), “Amidation of highly methoxylated citrus pectin with primary amines”, *Carbohydr. Polym.*, **42**(4), 359.
- Sips, R. (1948), “On the structure of a catalyst surface”, *J. Chem. Phys.*, **16**(5), 490-495.
- Somya, A., Rafiquee, M. and Varshney, K.G. (2009), “Synthesis, characterization and analytical applications of sodium dodecyl sulphate cerium (iv) phosphate: A new pb (ii) selective, surfactant-based intercalated fibrous ion exchanger”, *Colloid. Surface. A Physicochem. Eng. Asp.*, **336**(1), 142-146.
- Suteu, D., Zaharia, C., Muresan, A., Muresan, R. and Popescu, A. (2009), “Using of industrial waste materials for textile wastewater treatment”, *Environ. Eng. Manage. J.*, **8**(5), 1097-1102.
- Tang, Q., Chu, J.M., Wang, Y., Zhou, T. and Liu, Y. (2016a), “Characteristics and factors influencing Pb(II) desorption from a Chinese clay by citric acid”, *Sep. Sci. Technol.*, **51**(17), 2734-2743.
- Tang, Q., Katsumi, T., Inui, T. and Li, Z.Z. (2015a), “Membrane behavior of bentonite-amended compacted clay towards Zn(II) and Pb(II)”, *Membr. Water Treat.*, **6**(5), 393-409.
- Tang, Q., Katsumi, T., Inui, T. and Li, Z.Z. (2015b), “Influence of pH on the membrane behavior of bentonite amended Fukakusa clay”, *Sep. Purif. Technol.*, **141**, 132-142.
- Tang, Q., Katsumi, T., Inui, T. and Li, Z.Z. (2014), “Membrane behavior of bentonite-amended compacted clay”, *Soil. Found.*, **54**(3), 329-344.
- Tang, Q., Tang, X.W., Hu, M.M., Li, Z.Z., Chen, Y.M. and Lou, P. (2010), “Removal of Cd(II) from aqueous solution with activated firmiana simplex leaf: Behaviors and affecting factors”, *J. Hazard. Mater.*, **179**(1-3), 95-103.
- Tang, Q., Tang, X.W., Li, Z.Z., Chen, Y.M., Kou, N.Y. and Sun, Z.F. (2009), “Adsorption and desorption behaviour of Pb(II) on a natural kaolin: Equilibrium, kinetic and thermodynamic studies”, *J. Chem. Technol. Biotechnol.*, **84**(9), 1371-1380.
- Tang, Q., Tang, X.W., Li, Z.Z., Wang, Y., Hu, M.M., Zhang, X.J. and Chen, Y.M. (2012), “Zn(II) removal with activated firmiana simplex leaf: Kinetics and equilibrium studies”, *J. Environ. Eng.*, **138**(2), 190-199.
- Tang, Q., Wang, H.Y., Tang, X.W. and Wang, Y. (2016b), “Removal of aqueous Ni(II) with carbonized leaf powder: Kinetics and equilibrium”, *J. Centr. South Univ.*, **23**(4), 778-786.
- Unuabonah, E.I., Adebowale, K.O. and Olu-Owolabi, B.I. (2007), “Kinetic and thermodynamic studies of the adsorption of lead (II) ions onto phosphate-modified kaolinite clay”, *J. Hazard. Mater.*, **144**(1-2), 386-395.
- USEPA, National Primary Drinking Water Regulations, EPA 816-F-09-0004, May 2009.
- Uslu, G. and Tanyol, M. (2006), “Equilibrium and thermodynamic parameters of single and binary mixture biosorption of lead (II) and copper (II) ions onto Pseudomonas putida: Effect of temperature”, *J. Hazard. Mater.*, **135**(1-3), 87-93.
- Wang, J. and Chen, C. (2014), “Chitosan-based biosorbents: modification and application for biosorption of heavy metals and radionuclides”, *Bioresour. Technol.*, **160**(5), 129-141.
- WHO (2011), *Guidelines for Drinking-Water Quality*, World Health Organization.
- Wong, K.K., Lee, C.K., Low, K.S. and Haron, M.J. (2003), “Removal of Cu and Pb by tartaric acid modified rice husk from aqueous solutions”, *Chemosphere*, **50**(1), 23-28.
- Xiong, C.H. and Yao, C.P. (2013), “Adsorption behavior of Cu(II) in aqueous solutions by SQD-85 resin”, *Iran. J. Chem. Chem. Eng.*, **32**(2), 57-88.
- Zhao, Y., Gu, F., Xu, J. and Jin, J. (2010), “Analysis of aging mechanism of SBS polymer modified asphalt based on Fourier transform infrared spectrum”, *J. Wuhan Univ. Technol. Mater. Sci.*, **25**(6), 1047-1052.
- Zhu, J., Tian, M., Zhang, Y., Zhang, H. and Liu, J. (2015), “Fabrication of a novel “loose” nanofiltration membrane by facile blending with chitosan-montmorillonite nanosheets for dyes purification”, *Chem. Eng. J.*, **265**, 184-193.

CC